Int J Thermophys (2015) 36:1699–1712
DOI 10.1007/s10765-015-1870-y

Toward Reliable Industrial Radiation Thermometry

Y. Yamada[1] · **J. Ishii**[1]

Received: 6 December 2013 / Accepted: 11 March 2015 / Published online: 18 April 2015

Abstract Application of radiation thermometry in industrial scenes is rapidly increasing with the widespread use of low-cost infrared thermometers and thermal imagers. However, their performances are not always up to the users' expectations. This is often due to lack of appropriate information on the limitations of the instrument performance and of radiation thermometry itself. In this article, these limitations are disclosed, namely the targeting capabilities of the thermometers including the size-of-source effect of thermal imagers, reflection errors, and unknown emissivity of the measurement object. Attempts made at the NMIJ are introduced, which aim at alleviating the effect of these difficulties. Two-color radiation thermometers have been neglected from the traceability chain and from standardization efforts due to their technical complexity. Recent activities to incorporate them effectively in the calibration chain and to establish international standards are presented. Calibration of low-cost thermometers with a fixed instrumental emissivity setting has been an issue for calibration laboratories. Simple apparatus that enables calibration of such instruments is described. Methods to compensate for unknown emissivities are presented utilizing auxiliary sources to realize a blackbody condition, which is applied to thermal imagers to overcome the problem of the size-of-source effect and reflection error at the same time. Extensions of the technique to objects with specular and scattering surfaces are described. Such efforts are encouraged in the thermometry community since they are essential in establishing an unbroken chain of traceability to the industrial front.

✉ Y. Yamada
y.yamada@aist.go.jp

[1] National Metrology Institute of Japan, National Institute of Advanced Industrial Science and Technology (AIST), Tsukuba 305-8563, Japan

Keywords Emissivity compensation · Emissivity setting · Infrared radiation thermometer · Size-of-source effect · Thermal imager · Two-color ratio thermometer

1 Introduction

In many industrial applications, temperature measurement holds the key to energy-efficient low-cost production of high-quality commercially competitive products often with added value. For instance, in steel production, temperature control is essential in every process, from the blast furnace where ore is reduced to produce iron, to such lines as coating lines where the final products are formed [1]. In the semi-conductor industry, from wafer production to device packaging, the needs for temperature measurement range from above 1000 °C to room temperature, with a measurement response time from tens of minutes to sub-millisecond [2]. Often in such industrial applications, contact measurement is not possible. However, in many of these processes, *in situ* implementation of radiation thermometry falls short of achieving the objective.

On the other hand, the number of commercial radiation thermometers is increasing in the market. This is due to the widespread use of low-cost infrared thermometers brought forth by improvement in thermal infrared sensor technology. Furthermore, due to reduced prices of two-dimensional infrared detectors, the market for thermal imagers is projected to grow rapidly in the near future [3]. Knowledge of the correct use that enables accurate measurement and awareness of the instruments' limitations in capability is becoming more and more important in the thermometer traceability chain as well as in the thermometer user community.

When applying a radiation thermometer to measurement at industrial sites, various obstacles are encountered. Examples of commonly observed difficulties are as follows:

(a) Difficulty in securing an unobstructed view of the target
The thermometer is required to view the object through a contaminated window glass of a viewing port, or through a narrow spacing, hardly enough to secure a clear sight of view.
(b) Small and moving objects
The object is smaller than the target area of the thermometer, such as a wire or particles, or is moving so that it does not always fully cover the target area.
(c) Calibration of instruments with fixed emissivity setting
Low-cost thermometers often have a fixed emissivity setting which cannot be changed to one for calibration with blackbody sources.
(d) Poor size-of-source effect
Low-cost infrared thermometers have a poor size-of-source effect, resulting in a large measurement error when viewing objects with a size different from the source size used for its calibration. Thermal imagers usually suffer errors of a greater magnitude from this effect.
(e) Reflection error
Ambient radiation is reflected on the non-blackbody object surface, which can be significant when the object temperature is close to or lower than the ambient temperature.

(f) Emissivity of measurement object unknown
The emissivity of the object depends not only on the object material but also on its surface condition, measurement wavelength, temperature, viewing angle, and polarization, and cannot be accurately known.

Admittedly, the above hardly covers all adversities that one meets. Temperature measurements of objects beneath running cooling water or behind thick mist or dust, of semi-transparent objects, or of inaccessible surfaces or sub-surfaces are only a few examples of such demanding circumstances.

In view of such global trends and current status, this article presents a summary of approaches taken by a metrology institute to tackle these issues. We describe performance limitations of low-cost infrared thermometers and thermal imagers, and attempts made at the National Metrology Institute of Japan to overcome the difficulties encountered in practice are presented, including development of novel calibration and measurement techniques as well as standardization efforts.

2 Two-Color Ratio Thermometry Standardization

A common solution to (a) and (b) of the above list of problems is to apply two-color ratio thermometry. By taking the ratio of the detected radiances at two wavelengths, wavelength-independent sources of error common to the two signals are canceled out, such as the ratio of the areas filled by the object within the field of view, window transmission loss due to dust, and loss by vignetting. However, two-color radiation thermometers are left out of the current industrial standardization activities, which successfully produced two international standard documents for single-wavelength radiation thermometers [4,5], and their traceability is often not as transparent as it should be.

In view of this, a working group was organized within the Temperature Measurement Subcommittee of Industrial Metrology Committee, Japan Society for the Promotion of Science, with the objective to clarify technical issues for specifying characteristics of two-color ratio thermometers and to draft an industrial specification document. The working group consists of members from thermometer manufacturers, the steel industry, universities, calibration laboratories, the Japan Atomic Energy Agency, and the NMIJ, AIST. Activities include a survey on the actual usage in industry and its problems, investigation on technical aspects required for standardization, preparation of a draft document for standardization, and considerations of proper traceability for two-color ratio thermometers. A draft industrial standardization document has been produced [6]. A simple example to illustrate the difficulty in this undertaking is how to define and characterize a "field of view." For a normal radiation thermometer detecting a single-wavelength band, this is the area that must be fully covered by the measurement object to obtain a correct temperature reading. For a two-color ratio thermometer, the object can be smaller than the field of view and it is still possible to obtain the correct reading. On the other hand, a radiation source within the field of view hotter than the measurement object can cause a large error, and therefore the field of view is the area that should be free of any interfering external sources. New definitions, concepts, and evaluation methods have been introduced in the document.

3 Calibration of Low-Cost Thermometers with Fixed Instrument Emissivity Setting

Low-cost infrared thermometers in the market very often have a fixed pre-set emissivity setting, for instance, of 0.95 or 0.98. This is of practical convenience for users who do not want to worry about adjusting the emissivity setting to match that of the object. However, this poses a problem for the calibration of the thermometer at the calibration lab: a reference blackbody source with an effective emissivity equal to one cannot be applied directly, and ideally a graybody source of emissivity equal to the thermometer setting is required.

Conveniently, a commercial planar radiation source with an effective emissivity of 0.95 is available for this purpose, and is widely applied. The question now is, what is the uncertainty of this emissivity? To investigate the situation quantitatively, measurements were conducted on the relative spectral radiance of the planar sources. A Fourier transform infrared spectrometer (FTIR) with a mercury cadmium telluride (MCT) detector was applied to measure the spectral radiance of two commercial planar radiation sources (manufacturer: Fluke Corp., Models: 4180 and 4181). A blackbody cavity source set at the same nominal temperature served as the reference, and the ratios of the spectral radiances of the planar radiation sources against the cavity source were evaluated. The results are shown for the wavelength range from 3 μm to 15 μm in Fig. 1a for the measurement with Model 4181 at temperatures of 100 °C, 300 °C, and 450 °C with the planar blackbody source effective emissivity setting of 0.95. In Fig. 1b the spectral radiance is compared for the two models at 100 °C for the same wavelength range. In the same graphs, spectral radiances of an ideal source with an emissivity of 0.95 are plotted as dashed lines for the same temperatures, taking into account the reflection effect from the room temperature ambient, which shows up as the tilt that becomes significant at lower temperatures and is more evident for longer wavelengths. The dashed lines have different tilts for different temperatures, indicating the complexity of corrections that needs to be applied if a blackbody source is used for calibration.

The devices have features to realize an effective emissivity of 1.0. Measurements of the spectral radiance ratio with this setting are also shown on the graphs for 450 °C (Model 4181) and 100 °C (Model 4180) along with that for an ideal blackbody source (dashed line).

As can be seen, unlike the ideal 0.95 emissivity sources (dashed lines) which show spectrally smooth profiles, the measured spectral radiance ratios given by the solid lines display a strong dip around 10 μm. The average spectral radiance for the range from 8 μm to 12 μm is approximately 0.95, but the quality of this approximation will depend on the spectral responsivity of the thermometer. The deviation, with an emissivity setting of one, from the spectral emissivity of an ideal blackbody source is seen to increase at shorter wavelengths. Unless the spectral range for the thermometer under calibration matches exactly that of the reference thermometer with which the planar radiation source has been calibrated, the uncertainty of calibration using this source is difficult to evaluate. Certainly, the device is not suitable for calibration of thermometers with nominal wavelengths other than the 10 μm range.

In order to enable calibration of thermometers with fixed emissivity settings using well-characterized cavity blackbody sources, new methods to realize neutral density

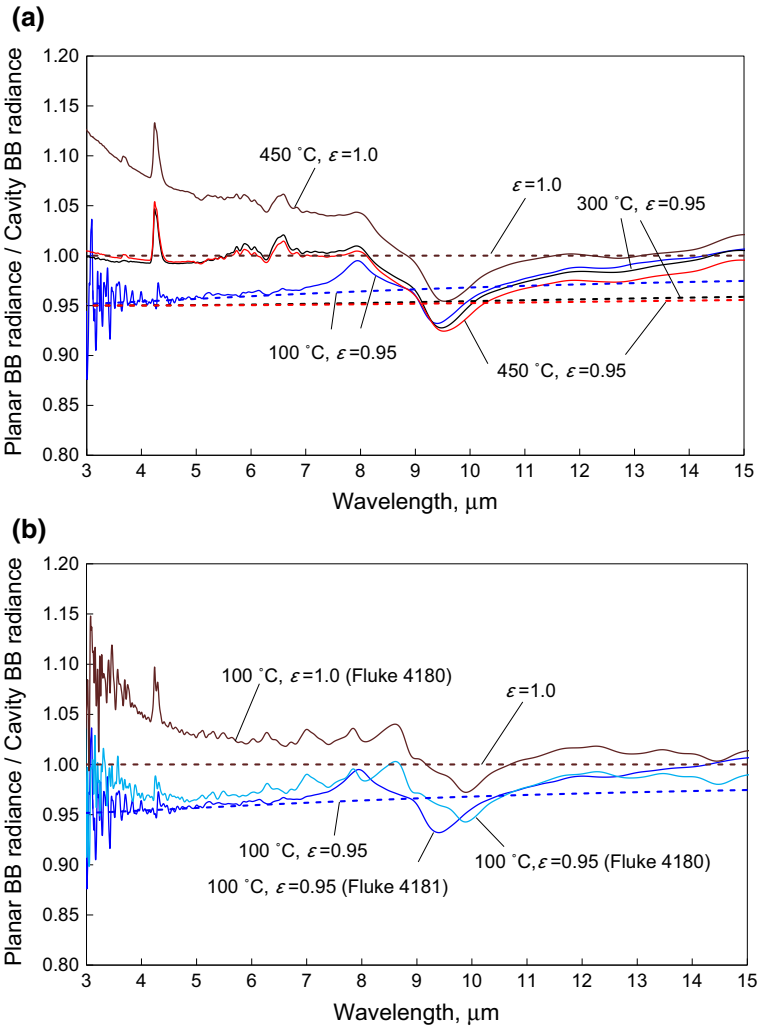

Fig. 1 Relative spectral radiance of planar radiation sources with nominal emissivity set to 0.95 and 1.0: (a) temperature dependence (Model 4181) and (b) measurement at 100 °C for the two models

filters of prescribed high transmittances such as 0.95 or 0.98 have been devised. Such filters can be placed in the optical path of the thermometer viewing the blackbody cavity with an emissivity of one, and the thermometer reading can be calibrated directly by the blackbody temperature monitored by a reference thermometer. A method to realize such a high transmittance neutral density filter is to make use of rotor blades with a relative opening area matching the filter transmittance. The blades will intermittently obscure the path of sight of the thermometer, but if the blades are rotated sufficiently faster than the response time of the thermometer, the rotor blades will appear to the thermometer as an attenuating filter with high transmittance with no spectral dependence. The thermometer will detect emitted and reflected thermal radiation from the

blade surface, but as long as the blades are at the same temperature as the ambient, it should not matter if the blade surface facing the thermometer is reflecting or absorbing, and the contribution will be equivalent to that of the reflection of the ambient radiation at a graybody target surface. The technique is presented in detail in [7].

4 Measurement Errors with Thermal Imagers

4.1 Size-of-Source Effect (SSE)

A majority of low-cost infrared thermometers are severely affected by a poor SSE, leading to large errors in measurement as well as requiring attention in calibration [8]. Similarly, thermal imagers are known to be affected by a large SSE, typically with error magnitudes several times larger than for spot-measuring infrared thermometers. A measurement was performed to evaluate this effect.

A measurement was made with a thermal imager detecting the 7.5 μm to 13 μm wavelength range with a thermal detector with 640 × 480 pixel resolution with a field of view of 24° × 18° at the minimum focal distance of 0.3 m. A variable diameter aperture was placed in front of a blackbody cavity immersed in a liquid bath set to 100 °C, and the output of the thermal imager at a distance of 500 mm was recorded while varying the aperture size. Figure 2 describes the average temperature reading of the central approximately 1 mm area as the aperture diameter is varied. As can be seen, even at the maximum aperture size of 55 mm, the signal is still increasing.

To demonstrate how the SSE will affect detected temperatures in a thermal image, an image of a statically and uniformly heated printed circuit board (PCB) was taken, which is shown in Fig. 3a. In the figure, the radiance temperature of the PCB appears higher at the substrate resin, where the emissivity is high, and lower at the metal wires, where the emissivity is low. It should be noted that the thicker wire (marked "d" in the figure) appears colder than the thinner wires (marked "b"), and the thicker substrate part (marked "a") hotter than the thinner part (marked "c"). This is quantitatively confirmed in Fig. 3b, where the thermal profile along a line is depicted. Although the image seams resolved from the imaging point of view, i.e., the metal patterns on the substrate can be clearly identified, from a thermometry point of view, the temperature

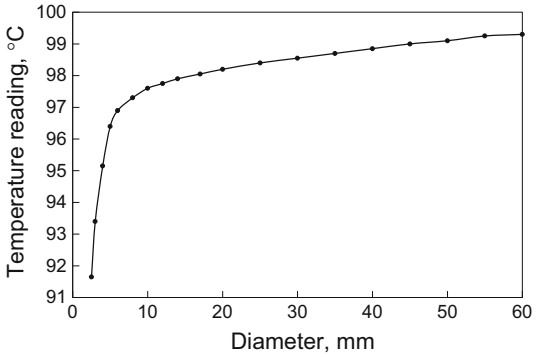

Fig. 2 SSE function of a thermal imager

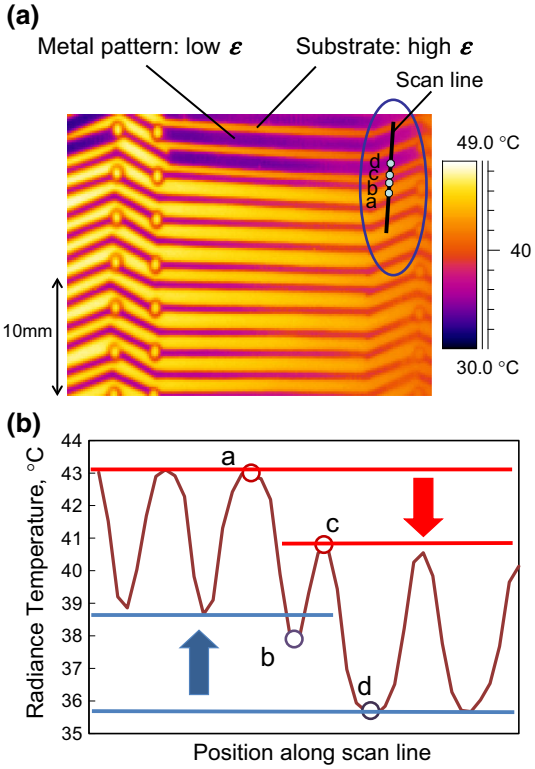

Fig. 3 Thermal image affected by SSE [10]: (a) image of a printed circuit board and (b) temperature profile along a line

reading in the image is affected by poor imaging quality through the SSE. For this instance, with a pattern dimension of the order of millimeters, the magnitude of the effect amounts to a few degrees.

4.2 Reflection Errors

Thermal images of a piece of PCB placed in a temperature-controlled container are shown in Fig. 4 for various container temperatures. The bucket-shaped container, made of stainless steel, was temperature regulated by water circulation in the side and bottom walls. The inside was purged with a slow flow of nitrogen to prevent condensation forming on the PCB surface. The images show that the apparently hot and cold parts are inverted depending on whether the object temperature is above or below ambient temperature. This is due to the ambient thermal radiation entering the container from the top opening and reflecting on the PCB low emissivity (=high reflectance) metallic parts. The reflection effect on the low emissivity part is seen to be in excess of 10 °C in the case of a 0 °C object temperature and can increase at lower temperatures.

Such reflection errors are present not only in thermal imagers but also in spot-measuring infrared thermometers, and attention is required especially when measuring objects of below ambient temperature or below freezing.

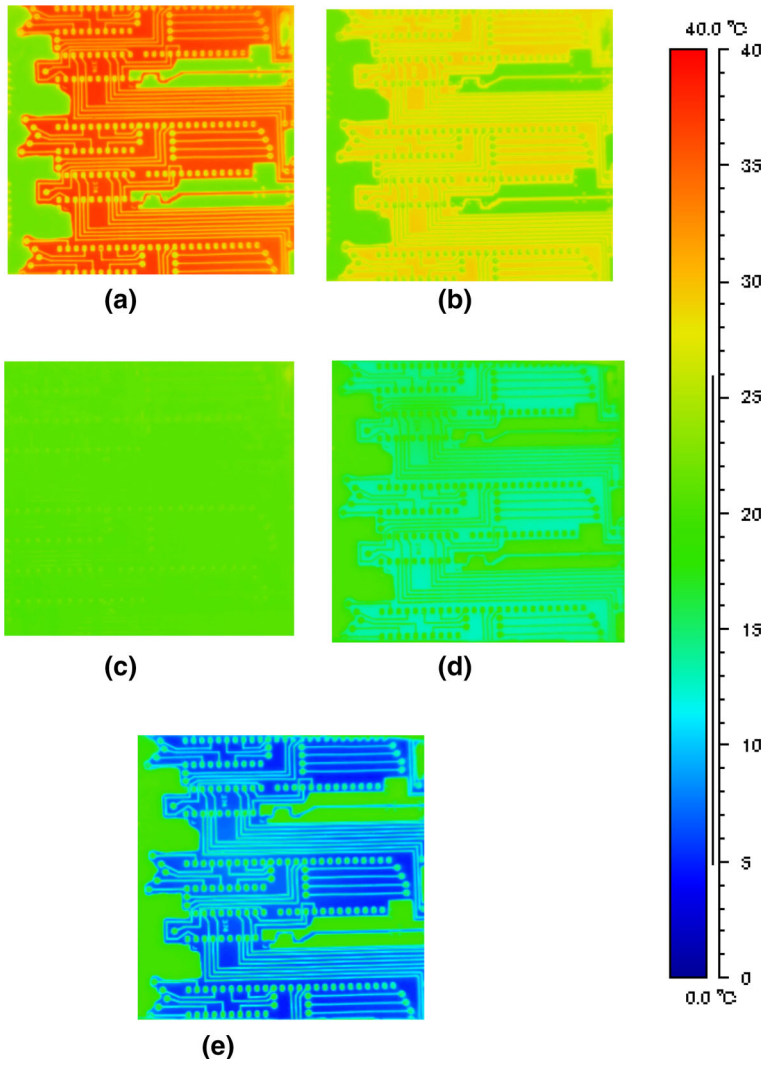

Fig. 4 Thermal image of a printed circuit board affected by ambient radiation. The ambient temperature is around 20 °C while the board temperature is varied as indicated: (a) 40 °C, (b) 30 °C, (c) 20 °C, (d) 10 °C, and (e) 0 °C

5 Unknown Emissivity

5.1 Emissivity-Pattern Reflectance-Ratio Radiation Thermometry

In Fig. 4c, it is found that at around room temperature, the pattern corresponding to the emissivity distribution disappears. This is because the sum of the thermal radiation originating from the print circuit board and the reflected ambient radiation at the board surface equals the blackbody radiation at that temperature, since the combined

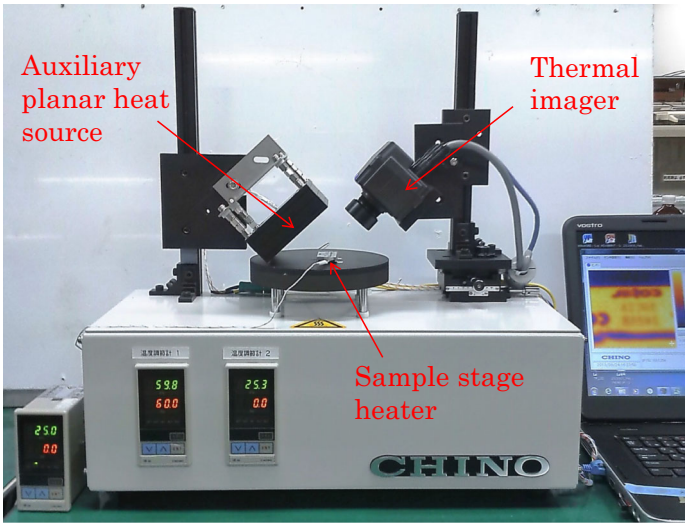

Fig. 5 Demonstration system for emissivity compensation with thermal imagers by emissivity-pattern reflectance-ratio method (Courtesy of Chino Corp.)

emissivity and reflectance equal one. It is therefore possible to tell from the absence of structure in the image that the object temperature is equal to ambient. The object temperature is obtained from the reading of the thermal imager with an emissivity setting of one. One can make use of this observation to realize emissivity-free radiation thermometry in the following way. Instead of varying the object temperature, as in Fig. 4, one can vary the ambient temperature and search for the condition for which the thermal image pattern disappears, and derive the object temperature from this image by assuming the emissivity equals one. This has been coined by the authors as "Disappearing pattern radiation thermometry" [9]. A demonstration system has been developed, which is shown in Fig. 5 [10]. A thermal imager views the object from an angle of 45° from the normal. An auxiliary planar thermal radiation source, placed opposite the thermal imager, acts as the source for variable ambient radiation. The object is heated from beneath. Measurement results are presented in [9,10].

The advantage of this method, in addition to being emissivity free, is that the measurement is SSE free, since there are no fine patterns in the image any more to affect the measurement. Furthermore, reflections of radiation from the background are an integral part of the measurement.

A disadvantage of this method is that adjustment of the auxiliary source temperature to match that of the object is time consuming. An alternative method is proposed to overcome this. In Fig. 6, the principle of the emissivity-free measurement is illustrated. In the figure, the detected radiance signal levels for the low and high emissivity parts move along the two tilted lines as the auxiliary source radiance is varied. The slopes of the two lines correspond to the reflectances of the parts, ρ_{Hi} and ρ_{Lo}. The "Disappearing pattern radiation thermometry" searches for the cross point of the lines by continuously varying the auxiliary source radiance. The alternative to this is to determine the cross point, i.e., the condition for pattern disappearance, from two thermal images taken at

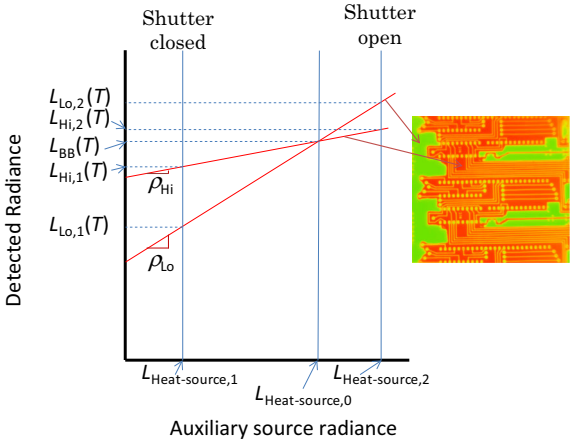

Fig. 6 Principle of emissivity-pattern reflectance-ratio radiation thermometry

two fixed auxiliary source temperatures, as depicted in Fig. 6. The two lines can be drawn by connecting the two points in the diagram derived by measurements at two different auxiliary source radiances, $L_{\text{Heat-source},1}$ and $L_{\text{Heat-source},2}$, for each part. This method carries on the features of the "Disappearing pattern radiation thermometry" plus the additional feature of fast response: the two images can be taken by rapidly switching between two source temperatures such as by opening and closing a shutter placed in front of the source. Furthermore, as long as the emissivity stays constant, the measurement with the auxiliary source needs to be done only once; after the two tilted lines are derived in Fig. 6, they can be shifted together to determine a new cross point whenever a new measurement at a different object temperature is made. Once determined, only the slopes of the tilted lines are relevant, or rather the ratio of the slopes since the auxiliary source radiance is not monitored. From this observation it has been named "Emissivity-pattern reflectance-ratio radiation thermometry."

Mathematical derivation of the above can be laid out as follows. The radiance detected by the thermal imager for the high emissivity $L_{\text{Hi},1}(T)$ and the low emissivity $L_{\text{Lo},1}(T)$ positions when the auxiliary source radiance is $L_{\text{Heat-source},1}$ can be written as below.

$$L_{\text{Hi},1}(T) = \varepsilon_{\text{Hi}} L_{\text{BB}}(T) + \rho_{\text{Hi}} L_{\text{Heat-source},1} \tag{1}$$

$$L_{\text{Lo},1}(T) = \varepsilon_{\text{Lo}} L_{\text{BB}}(T) + \rho_{\text{Lo}} L_{\text{Heat-source},1}. \tag{2}$$

Here $L_{\text{BB}}(T)$ is the blackbody radiance at temperature T, the temperature of the object. Then, the auxiliary source radiance level is changed to $L_{\text{Heat-source},2}$ and the same measurements are made

$$L_{\text{Hi},2}(T) = \varepsilon_{\text{Hi}} L_{\text{BB}}(T) + \rho_{\text{Hi}} L_{\text{Heat-source},2} \tag{3}$$

$$L_{\text{Lo},2}(T) = \varepsilon_{\text{Lo}} L_{BB}(T) + \rho_{\text{Lo}} L_{\text{Heat-source},2}. \tag{4}$$

From Eqs. 1 to 4, and taking into account the relations, $\varepsilon_{\text{Hi}} + \rho_{\text{Hi}} = 1$ and $\varepsilon_{\text{Lo}} + \rho_{\text{Lo}} = 1$, which follow from Kirchhoff's theorem, the blackbody radiation can be rewritten as

$$L_{\mathrm{BB}}(T) = \frac{L_{\mathrm{Hi},1}(T) - R_\rho L_{\mathrm{Lo},1}(T)}{1 - R_\rho} = \frac{L_{\mathrm{Hi},2}(T) - R_\rho L_{\mathrm{Lo},2}(T)}{1 - R_\rho}, \tag{5}$$

where

$$R_\rho \equiv \frac{\rho_{\mathrm{Hi}}}{\rho_{\mathrm{Lo}}} = \frac{L_{\mathrm{Hi},1}(T) - L_{\mathrm{Hi},2}(T)}{L_{\mathrm{Lo},1}(T) - L_{\mathrm{Lo},2}(T)} \tag{6}$$

is the reflectance ratio of the high and low emissivity positions of focus. From Eq. 5, it is possible to determine the true temperature T from $L_{\mathrm{BB}}(T)$ assuming a blackbody.

The method has the additional feature that, in principle, the auxiliary heater needs to be turned on only once to determine the reflectance ratio before the temperature measurement, eliminating risk of the heat from the heater affecting the target temperature. Ideally the auxiliary heater needs to be large enough to surround the target so that the differing angles of reflectance due to object surface roughness will not affect the measurement. In practice, this is not entirely possible, and whether there is the effect of the limited heater size or not needs to be confirmed case by case. The method is expected be a useful tool for any application of thermal imagers where the object has unknown and distributed emissivity, such as electronic devices.

5.2 Dual-Polarization Reflectance-Ratio Radiation Thermometry

A drawback of the above method is that its application is limited to objects with emissivity patterns. An alternative emissivity compensation technique has been devised using the difference in emissivity at two orthogonal polarizations [11]. When viewed from an inclined angle, a surface usually exhibits a different reflectance for light incident from air for the two polarizations, which for an opaque surface means that the emissivities are different. Both polarizations will have the same normal reflectance. For polarization perpendicular to the plane of incidence (s-polarization), the reflectance increases monotonically as the angle of incidence becomes inclined, and therefore the emissivity decreases monotonically. For polarization in the plane of incidence (p-polarization), reflectance would decrease with incident angle and, after reaching a minimum, turn to increase. For both polarizations the reflectance will approach 100 % at a 90° incident angle. Therefore, at a large angle of incidence, the emissivities for the two polarizations can differ by a large amount. The emissivities for the p- and s-polarizations can be written as $\varepsilon_{\mathrm{Hi}}$ and $\varepsilon_{\mathrm{Lo}}$, respectively, and the derivation given in Eqs. 1 to 6 can be applied. In this method, imaging is not required and the thermometer is a spot-detecting dual-polarization thermometer.

This "dual-polarization reflectance-ratio thermometry" has been applied successfully to *in situ* measurements in a millisecond high-temperature annealing process for semi-conductor wafers [2,11]. In this process, a 300 mm diameter silicon wafer is heated from the top side by a flash light from an array of xenon lamps. The thermometer views the center top side of the wafer from a port on the side wall. On another port on the opposite wall, the auxiliary source is installed. Thus, the arrangement is such that the angle of view has a large inclination and therefore is suitable for applying

this technique. It should be noted that, due to the specularity of the reflectance at the silicon surface even for wafers with patterns, a clear reflected image of the auxiliary source, which is large enough to cover the target size of the thermometer, is observed from the thermometer port.

5.3 Dual-Wavelength Reflectance-Ratio Radiation Thermometry

The dual-polarization method works well with objects with specular reflectance characteristics such as silicon wafers. However, with surfaces with scatter, large errors can be introduced due to the limited size of the auxiliary source which is insufficient to cover the wide scattering angle.

A new method has been proposed and tested. The method utilizes dual-wavelength detection instead of dual-polarization detection since the spectral emissivity is less sensitive to surface roughness than the polarized emissivity. The "reflectance-ratio" emissivity compensation can be applied with a minor modification [12]. We utilize an auxiliary source that can be turned on and off. The dual-wavelength thermometer, detecting the two wavelengths λ_1 and λ_2, generates two signals corresponding to the superimposed intensity detected at these wavelengths. Equations 1 to 4 can now be rewritten as follows:

$$L_{\lambda_1,\mathrm{Off}}(T) = \varepsilon_{\lambda_1} L_{\mathrm{BB},\lambda_1}(T) \tag{7}$$

$$L_{\lambda_2,\mathrm{Off}}(T) = \varepsilon_{\lambda_2} L_{\mathrm{BB},\lambda_2}(T) \tag{8}$$

$$L_{\lambda_1,\mathrm{On}}(T) = \varepsilon_{\lambda_1} L_{\mathrm{BB},\lambda_1}(T) + \rho_{\lambda_1} L_{\lambda_1,\text{Heat-source}} \tag{9}$$

$$L_{\lambda_2,\mathrm{On}}(T) = \varepsilon_{\lambda_2} L_{\mathrm{BB},\lambda_2}(T) + \rho_{\lambda_2} L_{\lambda_2,\text{Heat-source}}. \tag{10}$$

Here $L_{\lambda_1,\mathrm{Off}}(T)$ and $L_{\lambda_2,\mathrm{Off}}(T)$ are the detected radiance with the auxiliary source off, and $L_{\lambda_1,\mathrm{On}}(T)$ and $L_{\lambda_2,\mathrm{On}}(T)$ with the source on, for detected wavelengths λ_1 and λ_2, respectively. ε_{λ_1}, ε_{λ_2}, ρ_{λ_1}, and ρ_{λ_2} are the emissivities and reflectances of the surface at these wavelengths, and $L_{\lambda_1,\text{Heat-source}}$ and $L_{\lambda_2,\text{Heat-source}}$ are the auxiliary source radiances at the same wavelengths. $L_{\mathrm{BB},\lambda_1}(T)$ and $L_{\mathrm{BB},\lambda_2}(T)$ are the blackbody thermal radiances at temperature T.

From Eqs. 7 to 10 we can derive the blackbody radiance as follows:

$$L_{\mathrm{BB},\lambda_1}(T) = \frac{L_{\lambda_1,\mathrm{Off}}(T) - \alpha(T) R_\rho L_{\lambda_2,\mathrm{Off}}(T)}{1 - R_\rho}, \tag{11}$$

where

$$R_\rho \equiv \frac{\rho_{\lambda_1}}{\rho_{\lambda_2}} = \frac{L_{\lambda_1,\mathrm{On}}(T) - L_{\lambda_1,\mathrm{Off}}(T)}{L_{\lambda_2,\mathrm{On}}(T) - L_{\lambda_2,\mathrm{Off}}(T)} \Big/ R_{\mathrm{HS}} \tag{12}$$

and $\alpha(T) \equiv \frac{L_{\mathrm{BB},\lambda_1}(T)}{L_{\mathrm{BB},\lambda_2}(T)}$ is the radiance ratio at the two wavelengths of a blackbody at temperature T. R_{HS} is the heat source radiance ratio: $R_{\mathrm{HS}} \equiv \frac{L_{\lambda_1,\text{Heat-source}}}{L_{\lambda_2,\text{Heat-source}}}$, which can be monitored by the same dual-wavelength thermometer, if necessary, by intermittently changing the alignment. Note that only the ratio of the auxiliary source radiance is

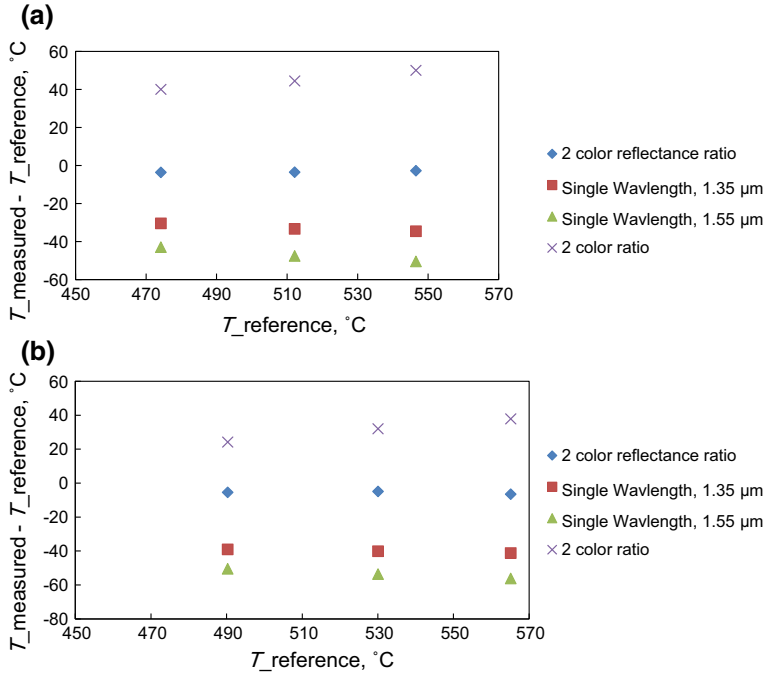

Fig. 7 Preliminary measurement result of dual wavelength reflectance-ratio radiation thermometry [12]

required. $\alpha(T)$ is a function of T, making the determination of T through Eq. 11 recursive. However, an initial estimated T can be applied for $\alpha(T)$, which can be used iteratively to determine T from the converged value.

A preliminary measurement with dual-wavelength reflectance-ratio radiation thermometry was performed. The objects were two stainless-steel plate samples with thicknesses of 4.9 mm and 9.4 mm, respectively, placed on a planar electrical resistive heater. One sample had a surface as drawn, while the other had a polished surface. Black paint was applied in the vicinity of the area that was scanned to give the reference temperature by measurement with the same thermometer assuming an emissivity of 0.95. The radiation thermometer had detecting wavelengths of 1.35 μm and 1.55 μm, and was equipped with a rotating mirror for linear scanning. A silicon carbide heater rod was placed parallel to the stainless steel sample surface to serve as the auxiliary linear radiation source. The result of the temperature measurement, evaluated as the difference from the measured reference temperature at the black paint, is shown in Fig. 7, for the dual-wavelength reflectance-ratio method, for single-wavelength thermometer measurements treating the two wavelengths individually without emissivity compensation (i.e., treating the emissivity as one), and by two-color ratio thermometry. The dual-wavelength reflectance-ratio method shows agreement within 4 K for the "as drawn" sample, and within 7 K for the "polished." This is in contrast to the result applying the conventional two-color ratio thermometry, which shows errors of tens of degrees. It is worth noting that the measurements were made in air, and therefore the sample surface

was oxidizing and changing color with time during the measurement, demonstrating the effectiveness of the technique for real-time emissivity compensation.

6 Conclusions

Low-cost infrared radiation thermometers and thermal imagers are becoming everyday tools in the industrial scene for temperature measurements. In this article difficulties encountered at the measurement site as well as in the calibration laboratories of such industrial thermometers have been addressed. Attempts made at the NMIJ have been presented, which aims to overcome these difficulties: standardization of two-color ratio thermometers, high transmittance neutral density filters for calibration of thermometers with fixed emissivity setting, and emissivity compensation techniques by the reflectance-ratio method for spot thermometers and thermal imagers.

With the widespread use of the thermometers, the importance of user awareness to these difficulties and the adoption of appropriate methods to overcome them is increasing. The presented methods are far from solving all problems at the application site. Further efforts in the search of innovative ways to alleviate the effect of various adversities are highly desired.

Acknowledgments The authors gratefully acknowledge the assistance of P. Saunders of MSL for providing useful information regarding calibration of low-cost infrared thermometers, and Y. Kaneko and Y. Wang of the NMIJ for performing the measurements. The assistance of T. Iwasaki of Chino Corp. is also acknowledged for conducting measurements on special request.

References

1. T. Iuchi, Y. Yamada, M. Sugiura, A. Torao, Thermometry in steel production, in *Radiometric Temperature Measurements. II. Applications*, chap. 4, ed. by Z. Zhang, B. Tsai, G. Machin (Elsevier, Amsterdam, 2009)
2. Y. Yamada, J. Ishii, Int. J. Thermophys. **32**, 2304 (2011)
3. S. Takazawa, in *Proceedings of the Infrared Array Sensor Forum 2013* (Ritsumeikan University, Kyoto, 2013) [in Japanese]
4. IEC/TS 62492-1 Ed 1.0, *Industrial Process Control Devices—Radiation Thermometers—Part 1: Technical Data for Radiation Thermometers* (International Electrotechnical Commission, Geneva, Switzerland, 2008)
5. IEC/TS 62492-2 Ed 1.0, *Industrial Process Control Devices—Radiation Thermometers—Part 2: Determination of the Technical Data for Radiation Thermometers* (International Electrotechnical Commission, Geneva, Switzerland, 2013)
6. Temperature Measurement Subcommittee of Industrial Metrology Committee, 2 Color Ratio Thermometer Working Group Interim Activity Report and Draft Standard (Japan Society for the Promotion of Science, Tokyo, 2015) [partly in Japanese]
7. J. Ishii, Y. Yamada, Int. J. Thermophys. 2015. doi:10.1007/s10765-015-1862-y
8. P. Saunders, in *Proceedings of Ninth International Temperature Symposium* (Los Angeles), *Temperature: Its Measurement and Control in Science and Industry*, vol. 8, ed. by C.W. Meyer, A.I.P. Conference Proceedings 1552 (AIP, Melville, NY, 2013), pp. 619–624
9. Y. Yamada, J. Ishii, Jpn. J. Appl. Phys. **50**, 11RE04 (2011)
10. T. Iwasaki, Y. Yamada, J. Ishii, T. Shimizu, S. Kadoya, in *Proceedings SICE Annual Conference 2013*, Nagoya (Society of Instrument and Control Engineers, Tokyo, 2013), pp. 380–384
11. Y. Yamada, T. Aoyama, H. Chino, K. Hiraka, J. Ishii, S. Kadoya, S. Kato, H. Kiyama, H. Kondo, T. Kuroiwa, K. Matsuo, T. Owada, T. Shimizu, T. Yokomori, Jpn. J. Appl. Phys. **49**, 04DA20 (2010)
12. Y. Yamada, J. Ishii, in *Proceedings SICE Annual Conference 2014*, Sapporo (Society of Instrument and Control Engineers, Tokyo, 2014), pp. 1918–1920